Pakistan Veterinary Journal

ISSN: 0253-8318 (PRINT), 2074-7764 (ONLINE)
DOI: 10.29261/pakvetj/2026.252

RESEARCH ARTICLE

Body Weight- and Age-Adjusted Reference Model for Septal Mitral Annular Plane Systolic Excursion in Healthy Dogs

Zhi-Jia Zheng[1, 2, 3], Ming-Huang Chang[2], Wei-Yau Shia[1], Wei-Ming Lee[1] and Cheng-Hung Lai[1*]

[1]Department of Veterinary Medicine, National Chung Hsing University, Taichung, Taiwan; [2]Department of Veterinary Medicine, National Chiayi University, Chiayi, Taiwan; [3]Veterinary Teaching Hospital, National Chiayi University, Chiayi, Taiwan.
*Corresponding author: chlai@dragon.nchu.edu.tw

ARTICLE HISTORY (26-731)

Received: June 25, 2026
Revised: August 15, 2026
Accepted: August 21, 2026
Published online: October 24, 2026

Key words:
Allometric scaling
Dog
Echocardiography
Longitudinal function
Mitral annular plane systolic excursion
Z-score

ABSTRACT

Mitral annular plane systolic excursion (MAPSE) is an M-mode index of left ventricular longitudinal systolic motion. In dogs, interpretation of raw MAPSE is affected by wide body size variation; and the independent effect of age after body weight adjustment has not been quantified. This study aimed to develop a body weight- and age-adjusted reference model for septal MAPSE and derive normalized indices. This two-center retrospective study included 180 client-owned healthy dogs examined between November 2016 and December 2023. Inclusion criteria included the absence of structural cardiac abnormalities, sinus rhythm, systolic blood pressure <140mmHg, and no clinically relevant thoracic radiographic, hematologic, or biochemical abnormalities. Septal MAPSE was measured by M-mode echocardiography from the apical four-chamber view and averaged over three cycles. Multiple linear regression modeled $\log_{10}$(MAPSE), using $\log_{10}$(body weight) and age. Heart rate and sex/neuter status were assessed as additional covariates, and study center was assessed for systematic center-related differences. Model-based Z-scores and percentage of predicted MAPSE values were calculated. The final model was $\log_{10}(\text{MAPSE})=0.6279+0.3243\times \log_{10}(\text{BW})-0.008767\times\text{age}$, explaining 70.2% of variation in $\log_{10}$(MAPSE). Body weight and age were significant predictors ($P<0.0001$). Predicted MAPSE scaled allometrically with body weight and decreased by 2.0% per year. Z-scores and percentage of predicted MAPSE showed no residual association with body weight or age. Septal MAPSE in healthy dogs is body weight- and age-dependent. This model provides body weight- and age-adjusted expected values for interpreting septal MAPSE within the range represented by this cohort.

To Cite This Article: Zheng ZJ, Chang MH, Shia WY, Lee WM and Lai CH, 2026. Body weight- and age-adjusted reference model for septal mitral annular plane systolic excursion in healthy dogs. Pak Vet J, 46(10): 2628-2636. http://dx.doi.org/10.29261/pakvetj/2026.252

INTRODUCTION

Conventional echocardiographic indices such as fractional shortening and ejection fraction provide commonly used estimates of left ventricular (LV) systolic performance, but they have recognized limitations in dogs with myxomatous mitral valve disease (Morgan *et al.*, 2020) and do not specifically characterize longitudinal systolic motion (Wolf *et al.*, 2021). In dogs, methods for assessing LV longitudinal function include M-mode mitral annular plane systolic excursion (MAPSE), historically described as mitral annular motion in earlier canine study (Schober and Fuentes, 2001; Fukuzumi *et al.*, 2024), tissue motion annular displacement (Wolf *et al.*, 2018), pulsed-wave tissue Doppler imaging of the septal mitral annulus (Choi *et al.*, 2013), and other speckle-tracking–based indices (Dickson *et al.*, 2017). Although tissue motion annular displacement and global longitudinal strain provide quantitative assessments of LV longitudinal systolic function, they depend on adequate apical image acquisition, reliable tracking, dedicated software, and operator expertise (Mogensen *et al.*, 2025). These methods may be less feasible in emergency settings, due to time constraints, or in dyspneic, hemodynamically unstable, obese, or poorly cooperative dogs (Wolf *et al.*, 2018; Spalla *et al.*, 2019). Furthermore, breed-specific variations in thoracic conformation may further complicate image acquisition and analysis.

Similar limitations have been described in human echocardiography. Wang *et al.* (2023) noted that MAPSE

may be useful when image quality is poor because it does not require tracing of the entire LV endocardial border. In human critical-care cohorts, M-mode MAPSE has been evaluated as an indicator of LV systolic dysfunction and a prognostic marker in pediatric and adult septic shock (El-Zayat and Shalaby, 2018; Brault *et al.*, 2023), serving as a low-complexity adjunct when image quality is suboptimal or advanced techniques are unavailable (Wang *et al.*, 2023; Cirin *et al.*, 2024). Reproducibility data in pediatric echocardiography further indicate that M-mode-derived MAPSE possesses high intra- and interobserver reliability, with favorable reproducibility compared with B-mode derivations, even under challenging imaging conditions (Hensel *et al.*, 2018).

In healthy dogs, Schober and Fuentes (2001) provided reference data for M-mode mitral annular motion in three body weight groups (<15, 15–40 and >40kg), reporting a strong association with body weight and body surface area, a weak association with heart rate, and no significant association with age. However, categorical reference values and group-specific cut-off points do not provide the continuous body weight- and age-adjusted model for interpreting septal MAPSE in individual dogs. More recently, M-mode MAPSE and its ratio to left atrial volume have been evaluated as indices of ventricular filling pressure in dogs with myxomatous mitral valve disease (MMVD) (Perez *et al.*, 2026). In addition, a pilot study in dogs with mammary tumors reported reduced MAPSE and global longitudinal strain despite preserved conventional systolic indices, and evaluated age, body weight, heart rate, and normalized left ventricular dimension as covariates in exploratory models (Algan *et al.*, 2026). These emerging applications indicate that body weight and age should be considered when raw MAPSE values are interpreted in clinical populations.

Body size adjustment is a standard practice in canine echocardiography, given that M-mode and other cardiac linear measurements vary with body size and may differ among breeds, with many dimensions scaling allometrically rather than linearly across the wide range of canine body sizes (Esser *et al.*, 2020; Feldhütter *et al.*, 2022; Cerbu *et al.*, 2023; Treibert *et al.*, 2024). This approach has been extended to annular excursion indices, most notably tricuspid annular plane systolic excursion (TAPSE), for which body weight–dependent reference intervals and body weight–independent ratios have been established (Pariaut *et al.*, 2012; Caivano *et al.*, 2018; Visser *et al.*, 2018). Similar ratio-based approaches have also been used to derive body size–independent right-heart echocardiographic indices in dogs (Sankisov *et al.*, 2024). To date, a continuous body weight–adjusted model for septal MAPSE has not been reported in dogs.

Because age and other physiologic or demographic variables may also influence annular displacement, they must be considered in statistical modeling. A multicenter human reference study reported that M-mode MAPSE was associated with age, whereas 2D speckle-tracking–derived MAPSE was influenced by age, blood pressure, heart rate, and LV volume (Wang *et al.*, 2023). Similarly, canine studies of tissue motion annular displacement and longitudinal LV function have evaluated associations with body weight, age, heart rate, and sex (Dickson *et al.*, 2017; Wolf *et al.*, 2018). Breed-specific echocardiographic reference studies have also reported that body weight, age, sex, and breed may influence conventional echocardiographic measurements in dogs (Romito *et al.*, 2023; Favier *et al.*, 2025; Hu *et al.*, 2025). Therefore, when establishing a canine septal MAPSE reference model, body weight and age should be evaluated as primary covariates, with heart rate, sex, and neuter status considered as additional candidate physiologic or demographic covariates.

The objectives of this study were to develop a body weight- and age-adjusted reference model for septal MAPSE in healthy dogs and to derive model-based normalized indices. It was hypothesized that septal MAPSE would scale allometrically with body weight and decrease with age, and that model-based normalization would reduce residual dependence on these covariates.

MATERIALS AND METHODS

Study design and study population: This two-center retrospective observational study used a total of 1,520 de-identified medical records and archived echocardiographic data from client-owned dogs examined between November 2016 and December 2023 at National Chiayi University Veterinary Teaching Hospital, Chiayi city, Taiwan and Tianhe Animal Hospital, Taoyuan city, Taiwan, where examinations were performed as cardiac consultations. Dogs were included if they were clinically healthy based on available records and had no structural cardiac abnormalities on complete echocardiography, sinus rhythm, systolic blood pressure <140mmHg, no clinically relevant cardiopulmonary abnormalities on thoracic radiographs, and no clinically relevant abnormalities on hematology or serum biochemistry examinations. Records for dogs with congenital or acquired cardiac disease, non-sinus rhythm, systemic disease likely to affect cardiovascular function, incomplete clinical data, or images unsuitable for septal MAPSE measurement were excluded. Sex/neuter status, body weight, age, and heart rate of each dog were recorded.

Echocardiography and septal MAPSE measurement: All archived echocardiographic examinations had been performed by one experienced clinician in conscious, non-sedated dogs using a consistent clinical protocol with simultaneous electrocardiographic recording. Dogs were examined in right and left lateral recumbency, using a Toshiba Artida system with PST-30BT, PST-50BT, or PST-65AT probes, or a GE LOGIQ e system with a 3S-RS probe. Complete transthoracic echocardiography confirmed absence of structural cardiac disease before inclusion of the dog in the study. Septal MAPSE was measured by M-mode echocardiography from the left apical four-chamber view with the cursor aligned with the longitudinal motion of the septal mitral annulus. Septal MAPSE was defined as peak systolic displacement of the septal mitral annulus from end-diastole to end-systole, timed by electrocardiography, and averaged over three consecutive cardiac cycles (Schober and Fuentes, 2001).

Quality control and repeatability: Source M-mode images were retrospectively reviewed using predefined criteria, including cursor alignment, annular definition, and reliable identification of end-diastolic and end-systolic

annular positions. Measurements failing these criteria were excluded. Intra-observer repeatability was assessed in 20 dogs spanning the observed body-weight range. Septal MAPSE was remeasured from stored images by the same observer after a 2-week washout period while blinded to original values. Repeatability was evaluated using single-measure absolute-agreement intraclass correlation coefficient, coefficient of variation, and Bland–Altman analysis (Hensel et al., 2018; Wang et al., 2023). Interobserver variability and repeated image acquisition variability were not assessed, which represents a limitation of the study.

Statistical analysis: Statistical analyses were performed using MedCalc version 23.5.5. Continuous variables were assessed for normality with Shapiro–Wilk tests and are presented as mean ± SD, or median [with IQR] if approximately normal or non-normal; baseline range values are also provided. Categorical variables are presented as counts with percentages. All statistical tests were two-tailed, and $P<0.05$ was considered statistically significant. MAPSE and body weight were $\log_{10}$-transformed, and least-squares multiple linear regression modeled $\log_{10}$ (MAPSE) as a function of $\log_{10}$ (body weight) and age. Model assumptions were assessed using residual-versus-fitted plots, normal Q-Q plots, the Shapiro-Wilk test, and variance inflation factors. Observations with absolute standardized residuals >2.5 were reviewed against source images. Heart rate and sex/neuter category were evaluated as additional covariates after adjustment for $\log_{10}$ (body weight) and age. Sex/neuter category was entered as a four-level categorical variable, with intact females as the reference category. Study center was evaluated separately as a binary methodological factor, with the university veterinary teaching hospital coded as 0 and the primary-care animal hospital coded as 1. Predicted MAPSE, Z-score, percentage of predicted MAPSE, and approximate model-based conditional 95% intervals were calculated using the final model.

RESULTS

Study population: Of 181 initially eligible dogs, one was excluded during source-image quality review because the M-mode cursor was not aligned with the longitudinal motion of the septal mitral annulus, leaving 180 dogs for analysis. Age, body weight, heart rate, and septal MAPSE were not normally distributed, as shown by the Shapiro–Wilk test, and are summarized as median [IQR] with range in Table 1. The cohort was predominantly composed of smaller dogs: 123 dogs (68.3%) weighed <10kg, whereas 23 dogs (12.8%) weighed ≥20kg and only 4 dogs (2.2%) weighed ≥30kg. Twenty-two breed categories were represented; the most common were mixed-breed dogs, Poodles, Dachshunds, Maltese dogs, and Yorkshire Terriers. Sex-wise distribution of dogs was intact females, spayed females, intact males and castrated males (Table 1).

Regression model for septal MAPSE: The final regression model included $\log_{10}$(BW) and age as independent variables. Both predictors were significantly associated with $\log_{10}$(septal MAPSE). The equation was:

$$\log_{10}(MAPSE) = 0.6279 + 0.3243 \times \log_{10}(BW) - 0.008767 \times Age$$

where MAPSE is in millimeters, BW in kg, and age in years.

Table 1: Clinical and demographic characteristics of healthy dogs included in the final reference model (n = 180)

Continuous variables	Median [IQR]; range
Age (years)	9.0 [7–11]; 2–16
Body weight (kg)	6.25 [3.98–13.25]; 1.20–42.35
Heart rate (beats/min)	119.5 [103.0–139.5]; 55–215
Septal MAPSE (mm)	6.44 [5.44–8.10]; 3.40–13.64
Body weight category, n (%)	
<5kg	70 (38.9)
5 to <10kg	53 (29.4)
10 to <20kg	34 (18.9)
20 to <30kg	19 (10.6)
≥ 30kg	4 (2.2)
Sex/neuter status, n (%)	
Intact female	35 (19.4)
Spayed female	79 (43.9)
Intact male	26 (14.4)
Castrated male	40 (22.2)
Study center, n (%)	
University veterinary teaching hospital	38 (21.1)
Primary-care animal hospital	142 (78.9)
Breed distribution, n (%)	
Mixed-breed dog	38 (21.1)
Poodle	27 (15.0)
Dachshund	23 (12.8)
Maltese	19 (10.6)
Yorkshire Terrier	13 (7.2)
Other breeds	60 (33.3)
Breed categories (n)	22

Continuous variables are presented as median [IQR], because they were not normally distributed by the Shapiro–Wilk test. Categorical variables are presented as numbers (n) with % in parenthesis. IQR=Interquartile range; MAPSE = mitral annular plane systolic excursion.

The model accounted for 70.2% of the variation in $\log_{10}$(MAPSE) (R^2=0.7015, adjusted R^2=0.6982; F=208.02 with 2 and 177 degrees of freedom, P<0.0001). The residual SD was 0.06866 on the $\log_{10}$ scale. Regression coefficients are shown in Table 2. The body-weight coefficient corresponded to a 25.2% increase in predicted septal MAPSE for each doubling of body weight. The age coefficient corresponded to a 2.0% decrease in predicted septal MAPSE per year after adjustment for body weight. The back-transformed prediction equation was:

$$MAPSE_{pred} = 10^{(0.6279 + 0.3243 \times \log_{10}(BW) - 0.008767 \times Age)}$$

or equivalently:

$$MAPSE_{pred} \approx 4.25 \times BW^{0.3243} \times 10^{(-0.008767 \times Age)}$$

Table 2: Final multiple linear regression model for $\log_{10}$ (septal MAPSE) in healthy dogs

Variable	Coefficient	SE	95% CI	t	P value
Intercept	0.6279	0.01949	0.5895 to 0.6664	32.22	< 0.0001
$\log_{10}$ (BW)	0.3243	0.01592	0.2929 to 0.3558	20.37	< 0.0001
Age (years)	−0.008767	0.001731	−0.01218 to −0.005351	−5.06	< 0.0001

BW=Body weight; MAPSE=Mitral annular plane systolic excursion; SE=Standard error; CI=Confidence interval. Final model: $\log_{10}(MAPSE) = 0.6279 + 0.3243 \times \log_{10}(BW) - 0.008767 \times$ age, where MAPSE is in millimeters, body weight is in kilograms, and age is in years. Model summary: n=180; R^2=0.7015; adjusted R^2=0.6982; residual SD=0.06866; F=208.02 with 2 and 177 degrees of freedom; P<0.0001.

Observed and model-predicted septal MAPSE values are shown in Fig. 1A (versus body weight) and Fig. 1B (versus age). Figure 1A shows the nonlinear increase in

predicted septal MAPSE with body weight and the lower predicted values at older ages. Figure 1B shows a decline in predicted septal MAPSE with increasing age at each representative body weight.

Normalized septal MAPSE indices: Model-based Z-scores were calculated as each residual divided by the residual SD of the final model (0.06866). The Z-score distribution was centered near zero (mean 0.00; SD 0.994; Fig. 2A), and the 2.5th to 97.5th percentile range was −1.94 to 1.73. After normalization, model-based Z-scores were not associated with body weight (r=0.04; 95% CI, −0.11 to 0.18; P=0.625; Fig. 2B) or age (r <0.001, P>0.99; Fig. 2C).

Percentage of predicted MAPSE was calculated as 100 × $MAPSE_{obs}/MAPSE_{pred}$. Because percentage of predicted MAPSE was not normally distributed, the median percentage of predicted MAPSE in healthy dogs was 100.1% [IQR, 91.1–110.7%]. Percentage of predicted MAPSE was not associated with body weight (Spearman's rho= −0.02; 95% CI, −0.16 to 0.13; P=0.841) or age (Spearman's rho= −0.02; 95% CI, −0.17 to 0.12; P=0.755).

Conditional model-based intervals: Approximate model-based conditional 95% intervals were calculated on the log_{10} scale using the residual SD of the final model and back-transformed to millimeters. For example, a 10kg, 11-year-old dog had a predicted septal MAPSE of 7.17mm and a model-based conditional 95% interval of 5.25–9.80mm. Model-based conditional 95% intervals across selected combinations of body weight and age are shown in Table 3.

Model diagnostics: Model diagnostics supported the final log-linear model used to derive predicted septal MAPSE values, model-based Z-scores, and approximate conditional 95% intervals. The residual-versus-fitted plot showed no obvious heteroscedasticity or systematic curvature, indicating no major evidence of model-form misspecification across the fitted range (Fig. 3A). Residuals were compatible with normality on the normal Q–Q plot and by the Shapiro–Wilk test (W=0.995, P=0.813; Fig. 3B). Variance inflation factors were 1.04 for log_{10}(BW) and 1.04 for age, indicating no relevant multicollinearity.

The single case excluded during source-image quality review showed M-mode cursor misalignment with the septal mitral annulus. Compared with the model including all 181 initially eligible dogs, exclusion of this technically unreliable measurement improved residual normality (Shapiro–Wilk P from 0.017 to 0.813) while leaving the direction and magnitude of the regression coefficients essentially unchanged.

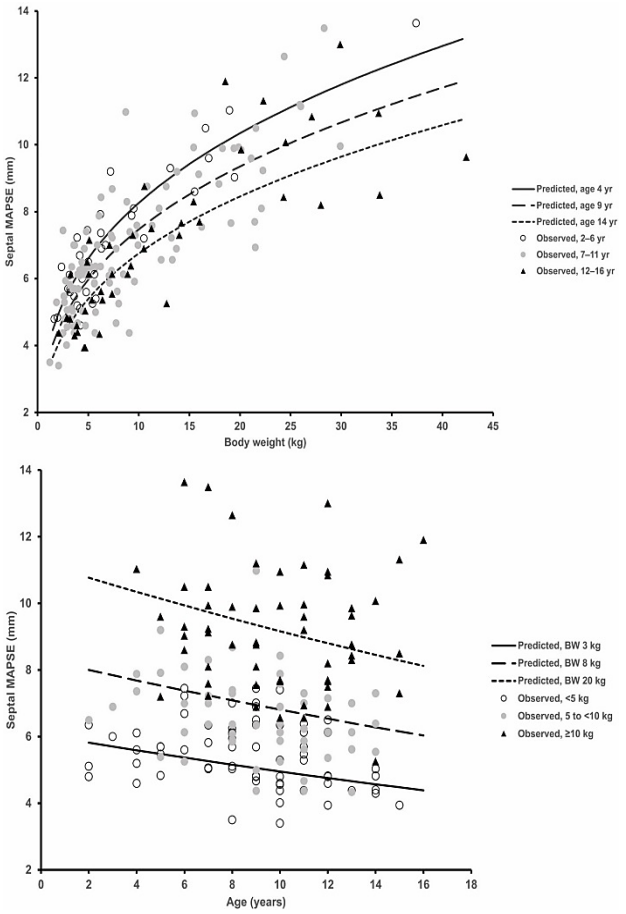


Fig. 1: Observed and model-predicted septal MAPSE in 180 healthy dogs. (A). Septal MAPSE plotted against body weight. Observed values are grouped by age category: 2–6 years, 7–11 years, and 12–16 years. Curves represent model-predicted septal MAPSE across body weight for the midpoint ages of these categories: 4, 9, and 14 years. (B). Septal MAPSE plotted against age. Observed values are grouped by body weight category: <5kg, 5 to <10kg, and ≥10kg. Lines represent model-predicted septal MAPSE across age for representative body weights of 3, 8, and 20kg. Predicted values were derived from the final regression model. MAPSE=Mitral annular plane systolic excursion; BW=Body weight.

Table 3: Predicted septal MAPSE and approximate model-based conditional 95% intervals in healthy dogs

Body weight (kg)	Age (Years)				
	2	5	8	11	14
2	5.10 (3.74–6.97)	4.80 (3.52–6.56)	4.52 (3.31–6.18)	4.26 (3.12–5.82)	4.01 (2.93–5.47)
3	5.82 (4.26–7.95)	5.48 (4.01–7.49)	5.16 (3.78–7.05)	4.86 (3.55–6.63)	4.57 (3.34–6.24)
5	6.87 (5.03–9.39)	6.47 (4.73–8.84)	6.09 (4.46–8.32)	5.73 (4.19–7.83)	5.39 (3.95–7.37)
8	8.00 (5.86–10.93)	7.53 (5.51–10.29)	7.09 (5.19–9.69)	6.67 (4.88–9.12)	6.28 (4.60–8.58)
10	8.60 (6.30–11.75)	8.10 (5.93–11.06)	7.62 (5.58–10.41)	7.17 (5.25–9.80)	6.75 (4.94–9.22)
15	9.81 (7.18–13.41)	9.24 (6.76–12.62)	8.69 (6.36–11.88)	8.18 (5.99–11.18)	7.70 (5.64–10.52)
20	10.77 (7.88–14.72)	10.14 (7.42–13.85)	9.54 (6.99–13.04)	8.98 (6.57–12.27)	8.45 (6.19–11.55)
25	11.58 (8.48–15.82)	10.90 (7.98–14.89)	10.26 (7.51–14.02)	9.66 (7.07–13.19)	9.09 (6.65–12.42)
30	12.29 (8.99–16.78)	11.56 (8.46–15.80)	10.88 (7.97–14.87)	10.24 (7.50–14.00)	9.64 (7.06–13.17)
35	12.92 (9.45–17.64)	12.16 (8.90–16.61)	11.44 (8.38–15.63)	10.77 (7.88–14.71)	10.14 (7.42–13.85)
40	13.49 (9.87–18.43)	12.69 (9.29–17.34)	11.95 (8.75–16.32)	11.25 (8.23–15.36)	10.59 (7.75–14.46)

Values are back-transformed model-predicted septal MAPSE in mm, with approximate model-based conditional 95% intervals in parentheses. Each predicted value represents the estimated conditional median, on the original scale for the specified body weight and age, rather than a sample median calculated from observed dogs. Predictions were calculated from the final model. Intervals were calculated on the log_{10} scale using the residual SD of the final model (0.06866) and back-transformed to mm. Selected combinations are within the marginal observed ranges of body weight (1.20–42.35 kg) and age (2–16 years). MAPSE=Mitral annular plane systolic excursion

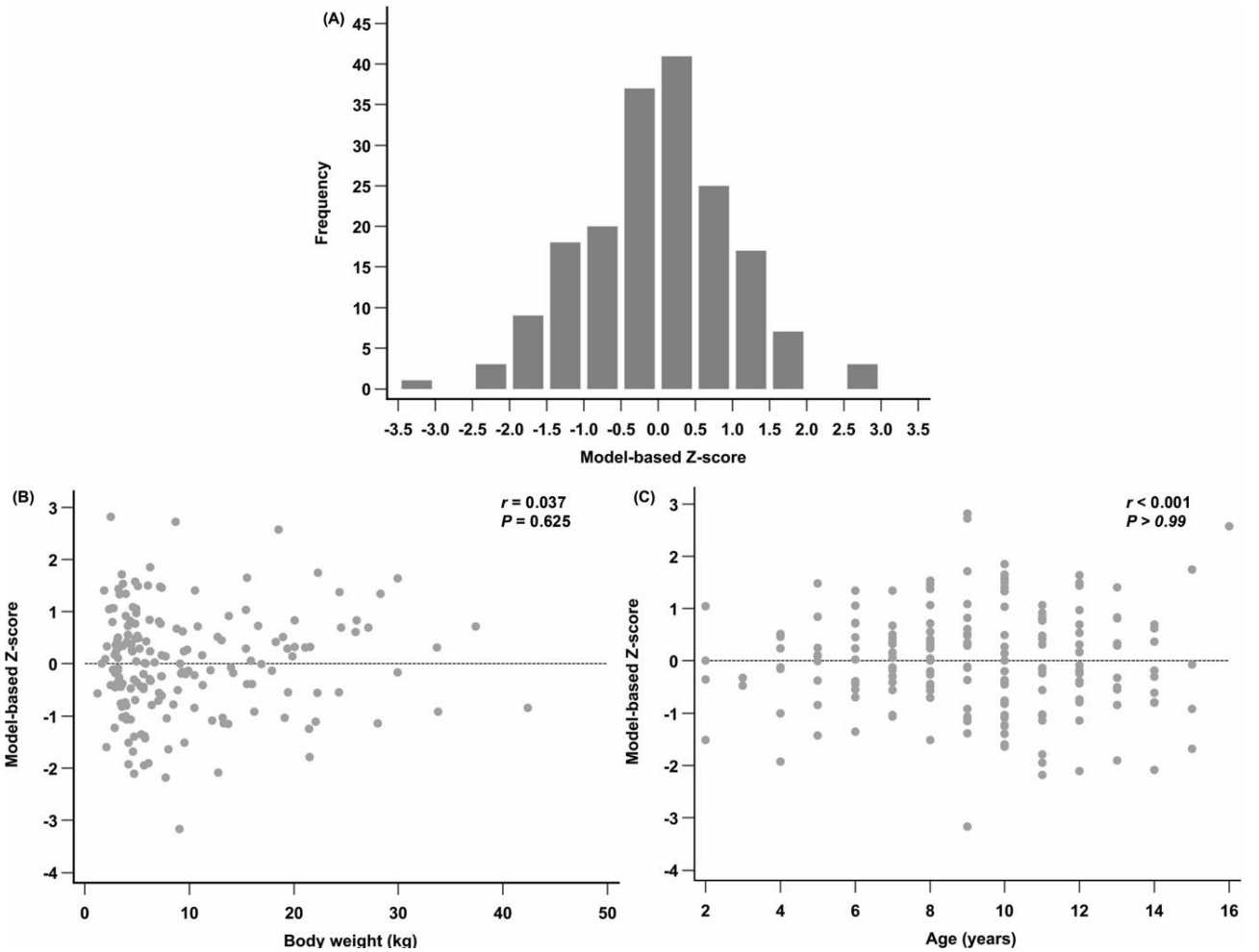


Fig. 2: Distribution and covariate independence of model-based septal MAPSE Z-scores in 180 healthy dogs. (A). Frequency distribution of model-based Z-scores. (B). Model-based Z-scores plotted against body weight. (C). Model-based Z-scores plotted against age. Z-scores were calculated from the final body weight- and age-adjusted regression model as the residual on the $\log_{10}$ scale divided by the residual SD of the final model. MAPSE=Mitral annular plane systolic excursion.

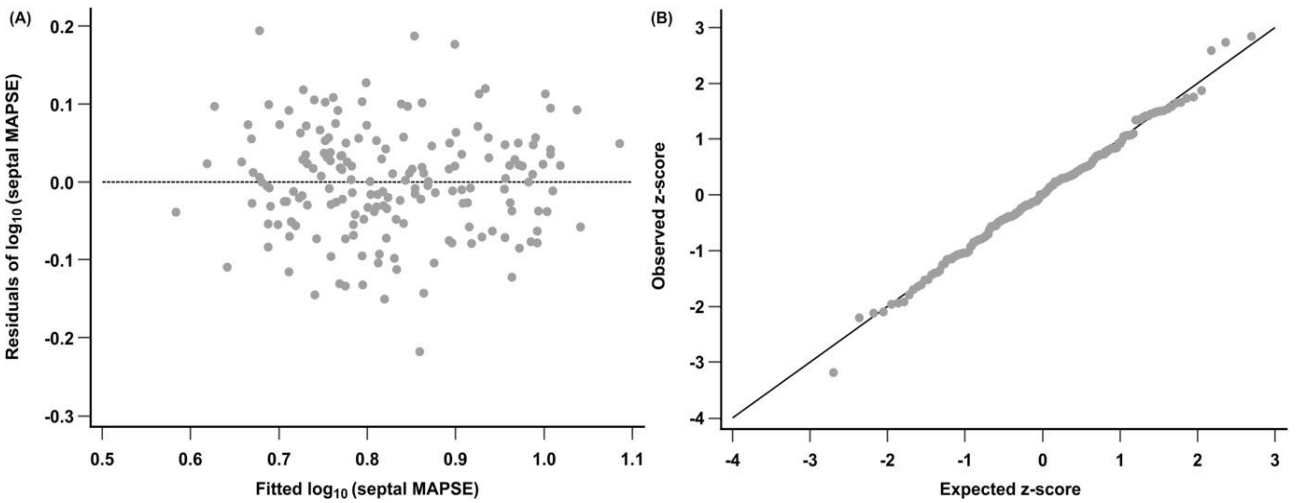


Fig. 3: Diagnostic plots supporting the final septal MAPSE regression model. (A). Residuals versus fitted values for the final multiple regression model. (B). Normal Q–Q plot of residuals, with expected (theoretical) z-scores on the X-Axis and observed z-scores on the Y-Axis. The residual-versus-fitted plot was used to assess heteroscedasticity or systematic curvature. The Q–Q plot was used to assess residual normality. MAPSE=Mitral annular plane systolic excursion.

Intra-observer measurement repeatability: In the repeatability subset (n=20), the single-measure absolute-agreement ICC was 0.96 (95% CI, 0.90–0.98), indicating excellent within observer stored-image remeasurement repeatability. The median intra-observer CV was 5.0% [IQR, 3.0–7.2%]. Bland–Altman analysis showed minimal mean bias between repeated measurements (MAPSE1−MAPSE2, −0.023mm; 95% CI, −0.370 to 0.325mm), with 95% limits of agreement from −1.476 to 1.431mm (Fig. 4).

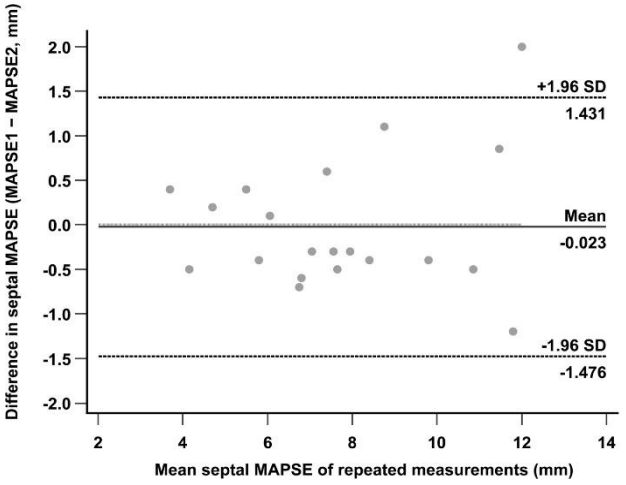


Fig. 4: Bland–Altman plot for intra-observer repeatability of septal MAPSE measurement from stored M-mode images. The difference between repeated measurements was calculated as MAPSE1 − MAPSE2 and plotted against the mean of the two measurements in 20 dogs. The solid line indicates the mean bias (−0.023mm), and dashed lines indicate the 95% limits of agreement (−1.476 to 1.431mm). MAPSE=Mitral annular plane systolic excursion.

Evaluation of additional covariates: Heart rate and sex/neuter category were evaluated after adjustment for $\log_{10}$(BW) and age. Heart rate was not associated with $\log_{10}$(MAPSE) (P=0.919). With intact females as the reference category, adjusted $\log_{10}$(MAPSE) did not differ for spayed females (P=0.454), intact males (P=0.719), or castrated males (P=0.222). Heart rate and sex/neuter category were therefore not retained in the final model.

Study center was evaluated separately to assess potential systematic center-related differences. With the university veterinary teaching hospital as the reference center, the coefficient for the primary-care animal hospital was 0.008755 after adjustment for $\log_{10}$ (BW) and age (P=0.491), indicating no evidence of a systematic center-related difference. The estimated coefficients for $\log_{10}$ (BW) and age were essentially unchanged, supporting the pooling of data from the two institutions.

DISCUSSION

This study established a body weight- and age-adjusted reference model for septal MAPSE in 180 healthy dogs. Septal MAPSE scaled allometrically with body weight and decreased by approximately 2.0% per year of age after adjustment for body weight. Heart rate and sex/neuter category did not improve model fit and were not retained. Study center was not associated with septal MAPSE after adjustment for body weight and age. Model-based Z-scores and percentage of predicted MAPSE showed no residual association with body weight or age within this healthy cohort.

Body weight was the dominant determinant of septal MAPSE, consistent with earlier canine M-mode mitral annular motion data (Schober and Fuentes, 2001). The allometric exponent of 0.3243 indicates that septal MAPSE increases with body weight in a nonlinear manner, and broad body weight categories or unadjusted reference values are unlikely to capture the relevant variation. The model is most robustly supported in dogs weighing <10kg, because this group accounted for 123 of 180 dogs (68.3%), whereas only 23 dogs (12.8%) weighed ≥20kg and only 4 (2.2%) weighed ≥30kg. Thus, the upper end of the allometric relationship was estimated from relatively few dogs. Cautious interpretation in larger dogs is also consistent with breed-specific data from Golden Retrievers, in which several left ventricular dimensions and volume-based indices differed from general canine reference values (Bagardi *et al.*, 2025).

The use of allometric scaling is consistent with current approaches to canine echocardiographic reference values. Cardiac linear measurements in dogs do not scale linearly with body weight (Cornell *et al.*, 2004), and large-scale reference studies have supported body weight–dependent prediction intervals for M-mode and volumetric left ventricular measurements (Esser *et al.*, 2020; Wess *et al.*, 2021). Similar strategies have been used for TAPSE, including body weight–dependent reference intervals (Pariaut *et al.*, 2012; Visser *et al.*, 2018) and body weight–independent ratios such as the TAPSE-to-aortic ratio (Caivano *et al.*, 2018). The present study applies the same principle to septal MAPSE as a longitudinal systolic index.

After accounting for body weight, age was also negatively associated with septal MAPSE; for a dog of a given body weight, the model predicted an approximately 2.0% lower septal MAPSE for each additional year of age. This finding differs from that of Schober and Fuentes (2001), who did not detect a significant association between mitral annular motion and age in healthy dogs. Continuous regression in a larger cohort, together with the broad age range of the present population, likely increased the ability to detect this modest age effect. More recent canine studies of longitudinal systolic function, together with human reference data, are consistent with a measurable age-related decline in longitudinal systolic indices (Dickson *et al.*, 2017; Wolf *et al.*, 2018; Wang *et al.*, 2023). These findings support the inclusion of age, in addition to body weight, when deriving expected septal MAPSE values.

Heart rate did not contribute to the model after adjustment for body weight and age, despite a wide observed heart rate range in conscious, non-sedated dogs. This may reflect that M-mode MAPSE primarily quantifies peak annular excursion rather than rate-dependent timing. In contrast, 2D speckle-tracking–derived MAPSE in human adults has been reported to be associated with heart rate (Wang *et al.*, 2023), which may be more sensitive to filling time and tracking quality than M-mode peak displacement. Sex/neuter category also did not improve model fit; however, the present design did not allow evaluation of stage of estrous cycle, age at neutering, or interactions with breed-specific cardiac geometry, which is a major limitation of this study.

Model-based Z-scores and percentage of predicted MAPSE help convert septal MAPSE from a raw displacement measurement into an observed-to-expected value adjusted for body weight and age. A raw MAPSE value in millimeters may be misleading when interpreted without considering the dog's size and age; after normalization, the same value can be judged according to its deviation from the value expected in healthy dogs. Percentage of predicted MAPSE expresses this deviation as an observed-to-expected ratio, whereas the Z-score expresses it on the residual scale of the model. In the

present cohort, both indices showed no residual association with body weight or age, indicating that model-based normalization removed the major covariate effects present in raw MAPSE. Z-scores are widely used in pediatric echocardiography to express deviation from size- or age-specific expected values on a standardized scale (Chubb and Simpson, 2012; Koestenberger *et al.*, 2012), and normalized TAPSE studies in dogs similarly support the clinical relevance of size-normalized annular excursion indices (Yuchi *et al.*, 2021).

Model diagnostics supported the use of the final log-linear model as the basis for predicted septal MAPSE values and the derived normalized indices. The absence of obvious systematic curvature in the residual-versus-fitted plot suggested that the log-linear model did not substantially overestimate or underestimate septal MAPSE across the fitted range. The absence of obvious heteroscedasticity suggested that residual variation was reasonably similar across predicted values, supporting the use of a common residual SD to calculate model-based Z-scores within the observed data range. These diagnostics therefore support the internal use of predicted MAPSE, percentage of predicted MAPSE, and Z-scores in this healthy cohort, although the conditional intervals reported here remain model-based approximations and should be interpreted cautiously, particularly at extreme body weight–age combinations.

In dogs with MMVD, conventional systolic indices can be difficult to interpret (Morgan *et al.*, 2020), and studies of MAPSE, annular excursion ratios, and longitudinal indices suggest that these measures may provide additional information (Wolf *et al.*, 2021; Perez *et al.*, 2026). A pilot study in dogs with mammary tumors also reported reduced MAPSE and global longitudinal strain despite preserved conventional systolic indices (Algan *et al.*, 2026). In routine clinical interpretation, the predicted MAPSE value provides an expected septal annular excursion for a dog of a given body weight and age, percentage of predicted MAPSE expresses how closely the observed value matches that expectation, and the model-based Z-score expresses the magnitude of deviation on a standardized scale. These indices may be useful when raw MAPSE is difficult to interpret because of body size or age, or when image quality is insufficient for global longitudinal strain, tissue motion annular displacement, or volumetric assessment. Because the model was derived exclusively from healthy dogs, low normalized septal MAPSE values should be interpreted together with other echocardiographic and clinical findings rather than used alone to diagnose LV systolic dysfunction. The absence of a disease cohort prevents estimation of diagnostic accuracy or disease-specific thresholds in the present study. Future prospective studies are needed to define the diagnostic accuracy of these indices.

Several limitations should be considered when interpreting results of the present study. Intra-observer repeatability was assessed in 20 dogs using stored M-mode images and suggested high within-observer agreement by ICC, with a mean CV of 5.0% and minimal mean bias on Bland–Altman analysis. This analysis was intended to assess the stability of septal MAPSE measurements used for model development, rather than to serve as a complete reproducibility study of MAPSE as a measurement technique. However, this repeatability analysis addressed stored-image remeasurement only, and the 95% limits of agreement indicated that repeated measurements in individual dogs could differ by approximately 1.4–1.5mm. Because only 20 dogs were included, this analysis should be considered a supportive rather than a complete reproducibility study. Although previous studies have reported good intra- and interobserver reproducibility for MAPSE measurements (Hensel *et al.*, 2018; Wang *et al.*, 2023), the present model was developed from measurements obtained by a single experienced observer using a consistent acquisition and measurement protocol. External validation is therefore needed to determine whether measurements obtained by other observers, from repeated image acquisition, or using other ultrasound systems can be applied to this model without systematic bias.

A further limitation is that circulating cardiac biomarkers, including N-terminal pro-B-type natriuretic peptide (NT-proBNP) and cardiac troponin I (cTnI), were not measured. Although biomarker data might have provided additional information regarding myocardial stress or injury, the lack of such data should be interpreted in the context of this retrospective clinical dataset, because such tests are not routinely available for all apparently healthy dogs and single biomarker measurements may have limited ability to rule out very early subclinical cardiac disease (Wolf *et al.*, 2013; Winter *et al.*, 2017). The most frequently represented breeds in this cohort—including Poodles, Dachshunds, Maltese dogs, and Yorkshire Terriers—are highly predisposed to MMVD; therefore, very early cardiac changes not yet apparent on echocardiography cannot be entirely excluded. Consequently, the age coefficient reported here should be interpreted as the association between age and septal MAPSE in echocardiographically healthy dogs, rather than as definitive evidence of purely physiological myocardial aging.

This was a retrospective study based on clinically acquired echocardiographic data from two hospitals and two ultrasound systems. Although study center was not associated with septal MAPSE after adjustment for body weight and age, study center was only a broad proxy for institutional and equipment-related effects and did not separately model ultrasound system effects. Therefore, residual equipment- or center-related variability cannot be excluded, and prospective studies using standardized acquisition protocols are warranted. Nevertheless, the absence of an adjusted center effect supports the use of the combined dataset for this model.

The body weight distribution was strongly skewed toward small-breed dogs. This skew toward smaller breeds should be considered when applying the model to larger dogs. In larger dogs, the model may still provide a useful estimate of expected septal MAPSE within the observed body weight range, but values should be interpreted with greater caution until additional data are available. This caution is consistent with breed-specific data from Golden Retrievers, in which several left ventricular dimensions and volume-based indices differed from general canine reference values (Bagardi *et al.*, 2025).

Breed-related effects could not be evaluated because only five out of 22 breed categories included more than

10 dogs, mixed-breed dogs (n=38), Poodles (=27), Dachshunds (n=23), Maltese dogs (n=19), and Yorkshire Terriers (n=13). Because breed, body weight, and body conformation are closely interrelated, the present study could not determine whether septal MAPSE differs among breeds after adjustment for body weight and age. Establishing breed- or somatotype-specific reference values, if clinically required, will require dedicated cohorts with sufficient numbers within each breed or breed group.

The model should not be extrapolated beyond the observed ranges of body weight (1.20–42.35kg) and age (2–16 years). Only septal MAPSE was measured; lateral MAPSE and averaged septal-lateral MAPSE were not analyzed and may have different relationships with body weight, age, and cardiac disease. Finally, the conditional model-based intervals reported here were approximate intervals calculated using the residual SD of the final model. Exact individual prediction intervals incorporating leverage may be slightly wider, particularly at extreme combinations of body weight and age.

Conclusions: Septal MAPSE in healthy dogs scaled allometrically with body weight and decreased by 2.0% per year of age after adjustment for body weight. The proposed model provides body weight- and age-adjusted expected values for interpreting septal MAPSE within the range represented by this cohort. These normalized indices may help clinicians recognize septal annular excursion that is lower than expected and should be interpreted together with other echocardiographic and clinical findings. Future studies in larger dogs, with additional observers or imaging systems, and in dogs with acquired cardiac disease will further define the range of clinical application and disease-specific interpretation.

Ethics statement: This was a retrospective observational study using de-identified clinical records and archived echocardiographic data from client-owned dogs examined for clinical reasons. All examinations and ancillary diagnostic tests had been performed as part of routine clinical evaluation, pre-anesthetic or wellness screening, or cardiac consultation, and no additional diagnostic or therapeutic procedures were performed for research purposes. De-identified records were reviewed retrospectively with permission from both institutions. No Institutional Animal Care and Use Committee or other animal ethics committee approval was required for this retrospective study using de-identified clinical data.

Authors contributions: ZJZ conceived and designed the study, performed original clinical echocardiographic examinations, retrospectively measured septal MAPSE from stored M-mode images, analyzed the data, and drafted the manuscript. MHC, WYS, WML, and CHL contributed to data interpretation and critical revision of the manuscript. CHL supervised the study. All authors read and approved the final manuscript.

Data availability: All data supporting the findings of this study are included in this manuscript. Further information may be obtained from the corresponding author upon reasonable request.

Conflict of interest: No potential conflict of interest is related to this manuscript.

Generative AI Statement: The authors declare that no Gen AI/DeepSeek was used in the writing/creation of this manuscript.

REFERENCES

Algan D, Varlik T, Tan H, *et al*., 2026. Preoperative cardiac risk stratification in dogs with mammary tumors using two-dimensional speckle tracking echocardiography: A pilot study. Animals (Basel) 16(9):1409. Doi: 10.3390/ani16091409.

Bagardi M, Ferrari P, Locatelli C, *et al*., 2025. Transthoracic echocardiographic reference intervals in 214 adult Golden retrievers. Journal of Veterinary Medical Science 87(4):356-363. Doi: 10.1292/jvms.24-0268.

Brault C, Zerbib Y, Mercado P, *et al*., 2023. Mitral annular plane systolic excursion for assessing left ventricular systolic dysfunction in patients with septic shock. British Journal of Anaesthesia Open 7:100220. Doi: 10.1016/j.bjao.2023.100220.

Caivano D, Dickson D, Pariaut R, *et al*., 2018. Tricuspid annular plane systolic excursion-to-aortic ratio provides a bodyweight-independent measure of right ventricular systolic function in dogs. Journal of Veterinary Cardiology 20(2):79-91. Doi: 10.1016/j.jvc.2018.01.005.

Cerbu M, Cerbu C and Papuc I, 2023. M-mode echocardiography in canine veterinary practice: a comprehensive review of left ventricular measurements in 44 different dog breeds. Animals (Basel) 13(18):2986. Doi: 10.3390/ani13182986.

Choi J, Kim H and Yoon J, 2013. Pulsed tissue Doppler imaging of the left ventricular septal mitral annulus in healthy dogs. Journal of Veterinary Science 14(1):85-90. Doi: 10.4142/jvs.2013.14.1.85.

Chubb H and Simpson JM, 2012. The use of Z-scores in paediatric cardiology. Annals of Pediatric Cardiology 5(2):179-184. Doi: 10.4103/0974-2069.99622.

Cirin L, Crisan S, Luca CT, *et al*., 2024. Mitral annular plane systolic excursion (MAPSE): A review of a simple and forgotten parameter for assessing left ventricle function. Journal of Clinical Medicine 13(17):5265. Doi: 10.3390/jcm13175265.

Cornell CC, Kittleson MD, Torre PD, *et al*., 2004. Allometric scaling of M-mode cardiac measurements in normal adult dogs. Journal of Veterinary Internal Medicine 18(3):311-321. Doi: 10.1892/0891-6640(2004)18<311:asomcm>2.0.co;2.

Dickson D, Shave R, Rishniw M, *et al*., 2017. Echocardiographic assessments of longitudinal left ventricular function in healthy English Springer spaniels. Journal of Veterinary Cardiology 19(4):339-350. Doi: 10.1016/j.jvc.2017.04.003.

El-Zayat RS and Shalaby AG, 2018. Mitral annular plane systolic excursion as a predictor of mortality in children with septic shock. Pediatric Critical Care Medicine 19(9):e486-e494. Doi: 10.1097/PCC.0000000000001661.

Esser LC, Borkovec M, Bauer A, *et al*., 2020. Left ventricular M-mode prediction intervals in 7651 dogs: population-wide and selected breed-specific values. Journal of Veterinary Internal Medicine 34(6):2242-2252. Doi: 10.1111/jvim.15914.

Favier D, Brugada-Terradellas C, Vernooij J, *et al*., 2025. Reference intervals for conventional transthoracic echocardiography and two-dimensional speckle tracking echocardiography-derived strain values in the Dutch Sheepdog ('Schapendoes'). Animals (Basel) 15(11):1524. Doi: 10.3390/ani15111524.

Feldhütter EK, Domenech O, Vezzosi T, *et al*., 2022. Echocardiographic reference intervals for right ventricular indices, including 3-dimensional volume and 2-dimensional strain measurements in healthy dogs. Journal of Veterinary Internal Medicine 36(1):8-19. Doi: 10.1111/jvim.16331.

Fukuzumi S, Mandour AS, Farag A, *et al*., 2024. Speckle tracking echocardiography for evaluation of myocardial functions before and after mitral valvuloplasty in dogs. Frontiers in Veterinary Science 11:1463889. Doi: 10.3389/fvets.2024.1463889.

Hensel KO, Roskopf M, Wilke L, *et al*., 2018. Intraobserver and interobserver reproducibility of M-mode and B-mode acquired mitral annular plane systolic excursion (MAPSE) and its dependency on echocardiographic image quality in children. PLoS ONE 13(5):e0196614. Doi.org/10.1371/journal.pone.0196614.

Hu T, Lin SL, Yang G, *et al*., 2025. Establishment of reference ranges for left heart echocardiography-related parameters in seven common small dog breeds in Taiwan and their relationships with body weight, age, and sex. Veterinary Radiology and Ultrasound 66(4):e70050. Doi: 10.1111/vru.70050.

Koestenberger M, Nagel B, Ravekes W, *et al*., 2012. Left ventricular long-axis function: Reference values of the mitral annular plane systolic excursion in 558 healthy children and calculation of z-score values. American Heart Journal 164(1):125-131. Doi: 10.1016/j.ahj.2012.05.004.

Mogensen JE, Bach MBT, Bay PG, *et al*., 2025. Speckle-tracking echocardiography in dogs: evaluating imaging parameters and methodological variability in global longitudinal strain assessment. Animals (Basel) 15(11):1523. Doi: 10.3390/ani15111523.

Morgan KRS, Monteith G, Raheb S, *et al*., 2020. Echocardiographic parameters for the assessment of congestive heart failure in dogs with myxomatous mitral valve disease and moderate to severe mitral regurgitation. The Veterinary Journal 263:105518. Doi: 10.1016/j.tvjl.2020.105518.

Pariaut R, Saelinger C, Strickland KN, *et al*., 2012. Tricuspid annular plane systolic excursion (TAPSE) in dogs: reference values and impact of pulmonary hypertension. Journal of Veterinary Internal Medicine 26(5):1148-1154. Doi: 10.1111/j.1939-1676.2012.00981.x.

Perez JM, Matos JI, Monge-Utrilla O, *et al*., 2026. Mitral annular plane systolic excursion to left atrial volume ratio as a novel index to assess ventricular filling pressure in dogs with myxomatous mitral valve disease. Veterinary Research Communications 50(4):287.

Romito G, Castagna P, Sabetti MC, *et al*., 2023. Echocardiographic values in healthy Pugs: effect of body weight, age, and sex. Open Veterinary Journal 13(8):965-976. Doi: 10.5455/OVJ.2023.v13.i8.2.

Sankisov JN, Visser LC, Davis KE, *et al*., 2024. Two-dimensional echocardiographic right heart ratios for assessment of right heart size in dogs: reference intervals and reproducibility. Journal of Veterinary Internal Medicine 38(6):3005-3015. Doi: 10.1111/jvim.17159.

Schober KE and Fuentes VL, 2001. Mitral annulus motion as determined by M-mode echocardiography in normal dogs and dogs with cardiac disease. Veterinary Radiology and Ultrasound 42(1):52-61.

Spalla I, Boswood A, Connolly DJ, *et al*., 2019. Speckle tracking echocardiography in cats with preclinical hypertrophic cardiomyopathy. Journal of Veterinary Internal Medicine 33(3):1232-1241. Doi: 10.1111/jvim.15495.

Treibert J, Friederich J, Fischer S, *et al*., 2024. Reference intervals for various measurements of canine left atrial size and function obtained using two-dimensional and three-dimensional echocardiography. Journal of Veterinary Cardiology 52:43-60. Doi: 10.1016/j.jvc.2024.02.005.

Visser LC, Sintov DJ and Oldach MS, 2018. Evaluation of tricuspid annular plane systolic excursion measured by two-dimensional echocardiography in healthy dogs: repeatability, reference intervals, and comparison with M-mode assessment. Journal of Veterinary Cardiology 20(3):165-174. Doi: 10.1016/j.jvc.2018.04.002.

Wang YH, Sun L, Li SW, *et al*., 2023. Normal reference values for mitral annular plane systolic excursion by motion-mode and speckle tracking echocardiography: a prospective, multicentre, population-based study. European Heart Journal - Cardiovascular Imaging 24(10):1384-1393.

Wess G, Bauer A and Kopp A, 2021. Echocardiographic reference intervals for volumetric measurements of the left ventricle using the Simpson's method of discs in 1331 dogs. Journal of Veterinary Internal Medicine 35(2):724-738. Doi: 10.1111/jvim.16089.

Winter RL, Saunders AB, Gordon SG, *et al*., 2017. Biologic variability of cardiac troponin I in healthy dogs and dogs with different stages of myxomatous mitral valve disease using standard and high-sensitivity immunoassays. Veterinary Clinical Pathology 46(2):299-307. Doi: 10.1111/vcp.12495.

Wolf J, Gerlach N, Weber K, *et al*., 2013. The diagnostic relevance of NT-proBNP and proANP 31-67 measurements in staging of myxomatous mitral valve disease in dogs. Veterinary Clinical Pathology 42(2):196-206. Doi: 10.1111/vcp.12044.

Wolf M, Lucina SB, Bruler BC, *et al*., 2018. Assessment of longitudinal systolic function using tissue motion annular displacement in healthy dogs. Journal of Veterinary Cardiology 20(3):175-185. Doi: 10.1016/j.jvc.2018.04.004.

Wolf M, Lucina SB, Silva VBC, *et al*., 2021. Assessment of longitudinal systolic function using tissue motion annular displacement in dogs with degenerative mitral valve disease. Journal of Veterinary Cardiology 38:44-58. Doi: 10.1016/j.jvc.2021.10.004.

Yuchi Y, Suzuki R, Teshima T, *et al*., 2021. Utility of tricuspid annular plane systolic excursion normalized by right ventricular size indices in dogs with postcapillary pulmonary hypertension. Journal of Veterinary Internal Medicine 35(1):107-119. Doi: 10.1111/jvim.15984.